

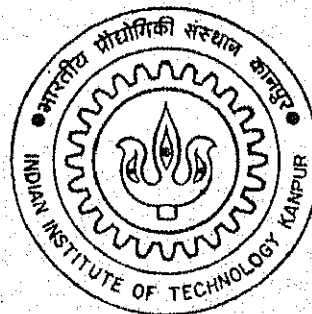
EXPERIMENTAL IMAGE RECONSTRUCTION
BY
CONVOLUTION BACKPROJECTION ALGORITHM

TH
NETP/1992/M

D9692

By

GYANENDRA KUMAR DWIVEDI



NUCLEAR ENGINEERING AND TECHNOLOGY PROGRAMME
INDIAN INSTITUTE OF TECHNOLOGY, KANPUR

April, 1992

NETP
1992
M
DWI
EXP

EXPERIMENTAL IMAGE RECONSTRUCTION

BY

CONVOLUTION BACKPROJECTION ALGORITHM

*A THESIS SUBMITTED
IN PARTIAL FULFILLMENT OF THE REQUIREMENTS
FOR THE DEGREE OF*

MASTER OF TECHNOLOGY

BY

GYANENDRA KUMAR DWIVEDI

TO THE

NUCLEAR ENGINEERING AND TECHNOLOGY PROGRAMME

INDIAN INSTITUTE OF TECHNOLOGY

KANPUR

APRIL, 1992

DEDICATED

TO MY

PARENTS

PCF&I

21 MAY 1992

CENTRAL LIBRARY

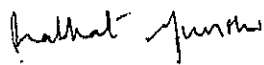
ACC. NO. **113494**

NETP-1992-M-DWI-EXP

CERTIFICATE

This is to certify that this work on " EXPERIMENTAL IMAGE
RECONSTRUCTION THROUGH CONVOLUTION BACKPROJECTION ALGORITHM" by
Gyanendra Kumar Dwivedi has been carried out under my supervision
and has not been submitted elsewhere for the award of a degree.

April 1992


Dr. Prabhat Munshi

Assistant Professor
Department of Mechanical Engg. &
Nuclear Engineering and Technology
I.I.T. Kanpur.

ABSTRACT

The image reconstruction techniques used widely in the areas of medical imaging has been successfully adapted to measure the void fraction and attenuation constant of the material. The convolution backprojection algorithm in conjunction with the Ramchandran-Laxminarayanan filter has been used for reconstruction in the form of a density distribution of a cross-section. The observation of the reconstructed results shows that the process of reconstruction is more vulnerable to uncertainties in the region close to the centre of the objects. The uncertainties arises due to the error incorporated in the projection data and the weaker sources.

ACKNOWLEDGEMENT

I wish to express my indebtedness to Dr.Prabhat Munshi for his invaluable guidance, his accessibility and unlimited co-operation during the course of study. It was due to his moral support that an uninitiated like me could attempt a project in this fascinating field.It was a nice experience to work under him.

I sincerely acknowledge the support of the entire NET family, especially Mr.S.S.Pathak for his invaluable guidance.

I am grateful to my family for consistently encouraging me despite the distance.

I can not forget the tasty meals I had, thanks to Mrs.Munshi. It certainly alleviated the monotony of the hostel food.

My sincere thanks to my friends and colleagues for the helpful discussions, inspiration and co-operation throughout my stay over here.

G.K.Dwivedi.

TABLE OF CONTENTS

Abstract	4
Acknowledgement	5
List of figures	8
List of symbols	9
1.0. Introduction	10
2.0. Preliminaries	12
2.1. Data collection modes	13
2.2. Parallel beam geometry	14
2.3. Fan beam geometry	16
2.4. Image inversion formula	18
2.4.1. Parallel beam formulation	18
2.4.2. Fan beam formulation	20
2.5. Convolution backprojection algorithm	22
2.5.1. Parallel beam algorithm	22
2.6. Radiation statistics	24
3.0. Experiment using single channel analyzer	27
3.1. Equipments needed	27
3.2. Description of equipments	27
3.2.1. Scintillation detector	27
3.2.2. Linear amplifier	31
3.2.3. High voltage unit	31
3.2.4. Low voltage unit	31
3.2.5. Single channel analyzer	31
3.2.6. Timer	32
3.2.7. Scaler	32
3.2.8. Gamma-ray source	32

4.0. Program implementation and description	34
4.1. Computer implementation of the CBP algorithm	34
4.2. Program for reconstruction of the image from data	36
5.0. Results	39
5.1. Data used	39
5.2. Results	40
6.0. Conclusion and recommendation	47
References	51
Appendix	
A. Data employed	53
B. Pictures of objects	57
C. Computer program for image reconstruction	62

LIST OF FIGURES

1. Parallel beam geometry	15
2. Fan beam geometry	17
3. Conversion of fan beam geometry to parallel beam geometry	23
4. Reconstructed image of object 1, scan 1	41
5. Reconstructed image of object 1, scan 2	42
6. Reconstructed image of object 2, scan 1	43
7. Reconstructed image of object 2, scan 2	44
8. Reconstructed image of object 3, scan 1	45
9. Reconstructed image of object 3, scan 2	46

LIST OF SYMBOLS

A	Fourier frequency;
B	Angle of extreme data-rays;
c	Chord of integration;
D	Distance of source from origin;
D_v	Partial derivative of $g(\sigma, \beta)$;
$f(r, \phi)$	Function being reconstructed;
$\tilde{f}(r, \phi)$	Reconstruction of $f(r, \phi)$;
$g(\sigma, \beta)$	projection data for fan beams;
l	Variable of integration;
Δl	Thickness of absorbing medium;
N	Radiation detector reading;
N_o	Radiation source strength;
$p(s, \theta)$	Projection data for parallel beam;
r, ϕ	Cylindrical co-ordinates;
s	Perpendicular distance of data from origin;
s'	s-distance of data-ray passing through (r, ϕ) ;
Δs	spacing between data-rays;
$W(F)$	Window function;
β	Source position(FAG);
θ	source position(PEG);
μ	absorption co-efficient.

CHAPTER 1

INTRODUCTION

Image processing has revolutionized the area of medical imaging, which is nowadays used in a variety of ways in non destructive testing(NDT), multi phase flow. Nuclear engineers have used image processing techniques in the measurement of void fraction during "LOSS OF COOLANT ACCIDENT". Because they are very reliable & accurate.

The experiments, which are performed by us using single channel analyzer(SCA), we measured cross-sectional distribution of the objects indirectly by probing the objects with the collimated invisible radiations and then interpret these results. We have related the measured data to the cross- sectional distribution in a known way. In the image reconstruction procedure, we processed the data to form the cross-sectional image i.e. interpreted the results indirectly. We take various strip integrals corresponding to a particular angle of view. This set of integrals is called a projection of the object. Given a number of such projections at different angles of view, the estimation of the corresponding distribution within the object is the basic problem of image reconstruction from projections.

The principles, which are used to reconstruct the image, are attributed to Radon[2], who proved that any arbitrary function could be recovered from its set of line integrals taken along various chords & directions. However, the method of Radon could not be implemented due to inherent mathematical complexities. Bracewell reported an application in radio astronomy and Cormack[3] derived an inversion formula, both of which were closer to being implemented as compared to Radon's solution. Bracewell & Riddle[12] and Ramchandran & Laxminarayana[9] showed how computations involved could be accelerated by adopting the use of convolutions.

The image processing can be used in diverse & wide ranging areas like astronomy & electron microscopy. We can use image scanners to estimate the quality of meat prior to slaughter. It can also be used to inspect wooden poles in power transmission.

The present study is an effort towards studying the image reconstruction through convolution backprojection algorithm which can be extended to various areas of applications.

CHAPTER 2

PRELIMINARIES

Single beam mono-energetic radiation attenuation phenomenon in a plane can be represented by

$$N = N_0 \exp[-\int_c \mu(r, \phi) dl] \quad (1)$$

The value of μ is characteristic of a material for a given type of radiation and the energy of radiation. Equation (1) considers μ to be a two-dimensional function of position, as the path of radiation is assumed to be restricted to a plane. The energy dependence of μ is also ignored. The simplifying assumption is valid for mono energetic radiation sources, e.g. γ -rays, and suitable corrections are incorporated to handle X-ray sources which have a distributed energy spectrum. We note that when the cross-section of interest has a uniform distribution of the absorbing material then (1) reduces to,

$$N = N_0 \exp (-\mu \Delta l), \quad (2)$$

where μ is no longer a function of position.

In general, any cross-section of interest will have non-uniform distribution. Rewriting (1) as,

$$p = \int_c \mu(r, \phi) dl \quad (3)$$

where

$$p = \ln(N_0/N)$$

We observe that recovering μ from the given data p is not a straightforward provision. Radon showed that it is possible to recover μ from a set of several p -values measured along various chords, c . These μ -values can then be suitably calibrated to give the density values if so desired.

2.1. DATA COLLECTION MODES: The image processing methodology requires attenuation data collected by an array of radiation detectors for the reconstruction of the function $\mu(r, \phi)$. Two popular data collection modes are termed as parallel-beam geometry (PBG) and fan beam geometry (FBG).

2.2. PARALLEL BEAM GEOMETRY: The IP scanners based on PBG mode have several pairs of radiation source and radiation detector systems which scan the object completely. Figure 1 depicts the configuration for a generic scanner. The source-detector pairs are spaced uniformly and the object to be imaged is stationed on a table which can be rotated to give different values of θ . The source-detector pairs are spaced uniformly and the object to be imaged is stationed on a table which can be rotated to give different values of θ . The line SD represents the path of the data ray. The perpendicular distance of the ray from the center of the object, which happens to be the origin of the frame of reference chosen for derivational and computational convenience, is denoted by s . Several SD pairs collect the data p for a given θ . This set of p is known as 'projection'. The object table is rotated to get several sets of p for different values of θ , i.e., different 'views'. The data thus collected is denoted by $p(S;\theta)$, the semi-colon indicating the procedure of data collection. If the object is stationary, then the SD system has to be rotated to collect the data for various 'views'.

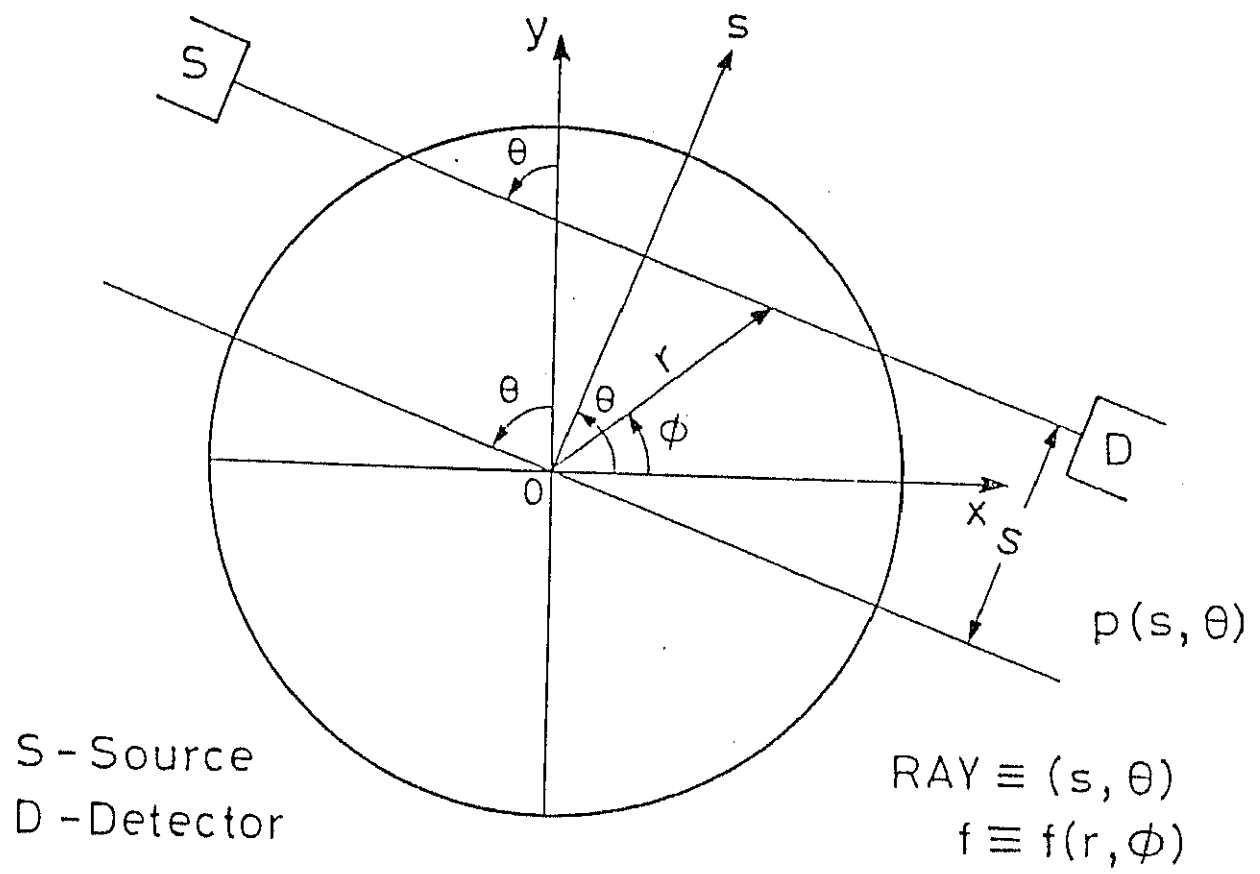


Fig. 1 Parallel beam collection geometry.

2.3.FAN BEAM GEOMETRY: The medical scanners incorporate the FBG collection mechanism which involves a rotating module including a source and an array of detectors stationed in an arc around the patient. Figure 2 shows the FBG configuration. Here, a single source views several detectors simultaneously and data are collected by different detectors corresponding to various angles, σ . This process is repeated for different values of β to get the IP data, $g(\sigma, \beta)$. The FBG mode can also be implemented for a rotating object system also. The data collection mechanism remains the same as that for the PBG case.

2.4.IMAGE INVERSION FORMULA: The process of reconstructing a two-dimensional function from its projection data is similar for the FBG and PBG cases. The parallel beam IP formulation involves Fourier transforms while the fan-beam formulation incorporates Hilbert transforms in the inversion process.

2.4.1.PARALLEL-BEAM FORMULATION: The inversion formula for the PBG case is based on the 'central-slice' theorem for Fourier transforms

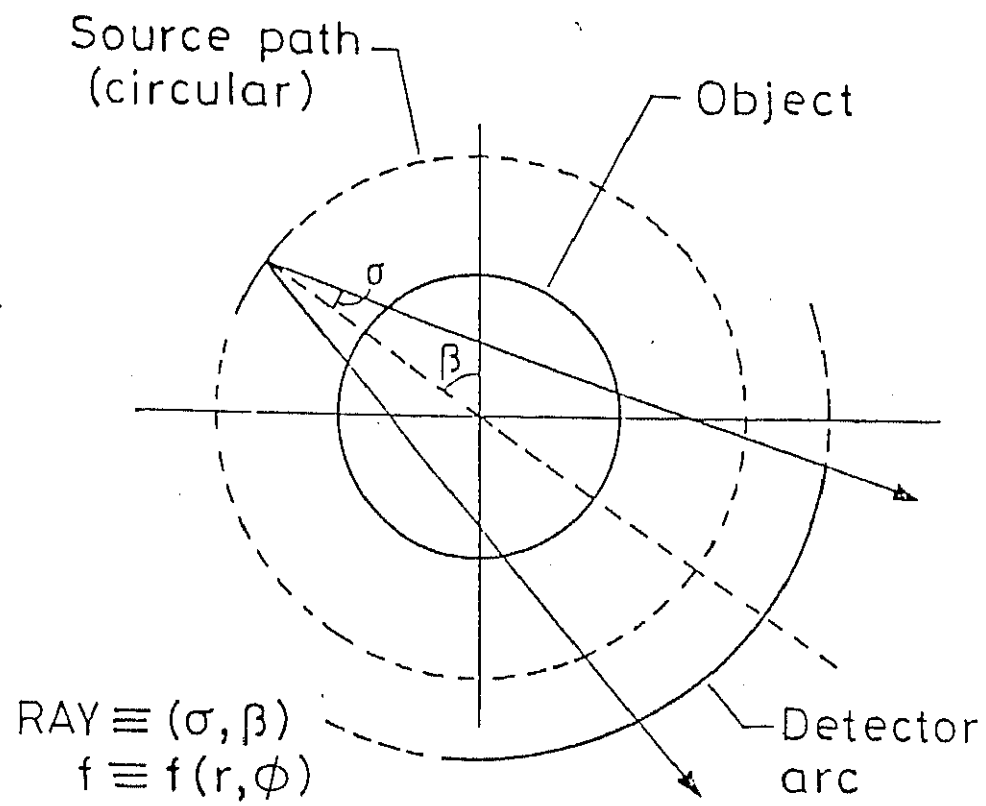


Fig. 2 Fan-beam data collection geometry.

of two-dimensional functions. The theorem states that the one-dimensional Fourier transform of the projection data, $p(s;\theta)$, with respect to the first variable s , is equal to the two-dimensional Fourier transform of the object function f being imaged. Mathematically,

$$\hat{f}(F;\theta) = p(F;\theta). \quad (5)$$

taking the inverse fourier transform of (5) we get

$$f(r,\phi) = \int_0^\pi \int_{-\infty}^\infty \hat{p}(F;\theta) \exp[-i2\pi F r \cos(\theta-\phi)] F dF d\theta. \quad (6)$$

Here for a given θ ,

$$\hat{p}(F;\theta) = \int_{-R}^R p(s;\theta) \exp[-i2\pi F s] ds \quad (7)$$

Equation (6) requires projection data on a continuous basis for all values of s and θ . For computational feasibility a finite cut-off is implemented in the form of a filter function, $W(F)$, which vanishes for $|F|$ greater than A , the cut-off frequency. Thus the filtered version of (6) becomes,

$$\tilde{f}(r, \phi) = \int_0^{\Pi} \int_{-\infty}^{\infty} \hat{p}(F; \theta) \exp[-i2\Pi F r \cos(\theta - \phi)] W(F) |F| dF d\theta. \quad (8)$$

Here, the reconstruction, \tilde{f} , is approximate due to the finite cut-off introduced in the computations. Also, the discrete nature of the IP data forces the practical implementation of A to be governed by the sampling theorem, i.e.,

$$A \geq [1/2\Delta s]$$

The band-limiting filter, introduced in electron micrography by Ramachandran & Laxminarayan is given by

$$W(F) = \begin{cases} 1, & |F| < A, \\ 0, & |F| \geq A, \end{cases}$$

and a popular 'sinc' filter used by Shepp & Logan is given by,

$$W(F) = \begin{cases} [\sin(\Pi F/2A)]/(\Pi F/2A), & |F| < A \\ 0, & |F| \geq A \end{cases}$$

2.4.2. FAN BEAM FORMULATION: The inversion formula for the FBG case was first derived by Herman & Naparstek and is given by,

$$\hat{f}(r, \phi) = (1/4\pi^2) \int_0^{2\pi} \int_{-B}^B [1/\sin(\sigma' - \sigma)] D_v g(\sigma, \beta) d\sigma d\beta,$$

where,

$$g(\sigma, \beta) = \text{data for the ray represented by } (\sigma, \beta),$$

$$D_v g(\sigma, \beta) = (1/U) [(\partial g / \partial \sigma) - (\partial g / \partial \beta)],$$

$$\sigma' = \tan^{-1} \{ [r \cos(\beta - \phi)] / [D + r \sin(\beta - \phi)] \},$$

$$U = \{ [r \cos(\beta - \phi)]^2 + [D + r \sin(\beta - \phi)]^2 \}^{1/2},$$

and other variables are as in the PBG case. We note that U is the distance of the radiation source from (r, ϕ) , the point being reconstructed, and σ' is the angular displacement of the particular data ray passing through that point (r, ϕ) . A major difference is the computation of partial derivatives of the data, g .

2.5.CONVOLUTION BACK PROJECTION ALGORITHM: The reconstruction algorithm based on the inversion formulae, are known as 'transform methods'. It is observed that these transform methods are slow and required very accurate interpolation schemes in computing the two-dimensional inverse fourier transforms. The introduction of convolutions eliminated the steps of computing the fourier transform of the data and the subsequent time consuming two-dimensional fourier inversion.

2.5.1.PARALLEL BEAM ALGORITHM: Exploiting the convolution property of fourier transforms,(8) becomes as,

$$\tilde{f}(r,\phi) = \int_0^R \int_{-\pi}^{\pi} p(s;\theta) q(s'_{-\theta}) ds d\theta \quad (10)$$

where,

$$q(s) = \int_{-A}^A W(F) |F| \exp[i2\pi F s] dF, \quad (11)$$

and,

$$s' = r \cos(\theta - \phi)$$

Here, q known as the convolving function and is the inverse fourier transform of the filter function, $W(F)$. Equations(10)-(11) are the fundamental equations of the convolution

back-projection(CBP) algorithm of IP. The inner integral of (10) is a convolution and the outer integral was termed back projection by the early researchers. The CBP algorithm is the most widely used method of reconstruction.

2.6.RADIATION STATISTICS:The quality of reconstruction is affected with four problems:

1:Due to errors in data collection process,

2:Due to the finite number of projections i.e., discretization of the problem,

3:Due to errors by numerical computations,

4:Due to statistical nature of photons, because of their interaction with the matter and the photon detector.

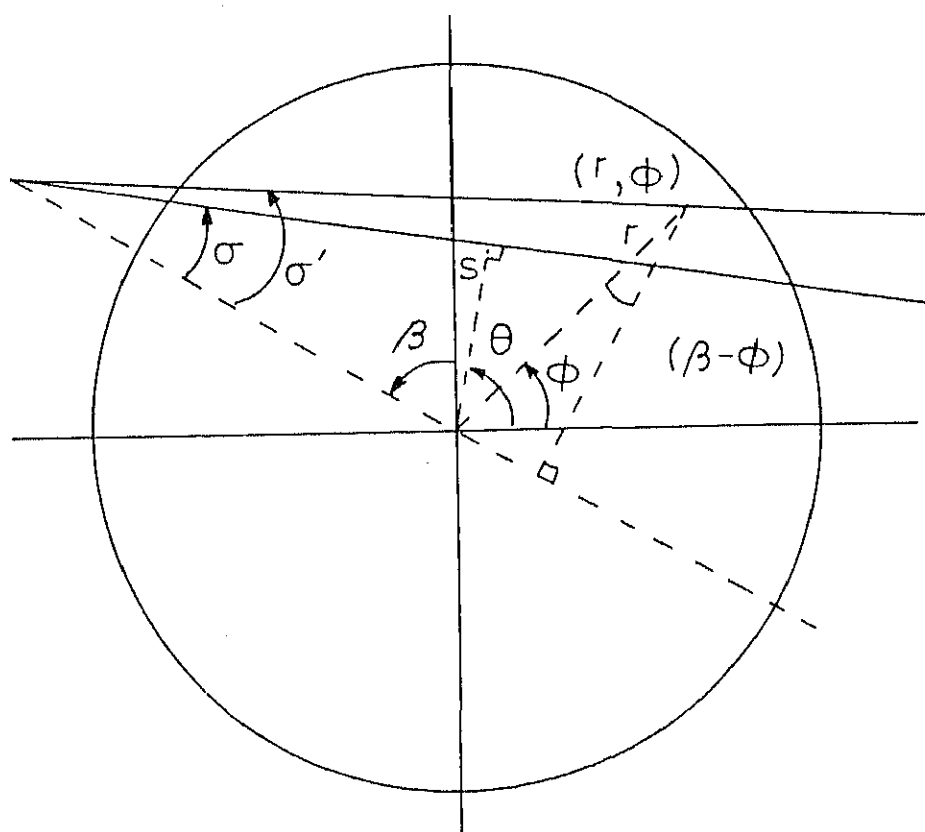


FIG. 3 CONVERSION OF FAN BEAM GEOMETRY TO
PARALLEL BEAM GEOMETRY

In gamma-ray image processing, the rays are generally monochromatic or at most, two wavelengths are presents. Due to this nature of gamma-ray, uneven detector response to the detector, and of beam hardening, which affects the X-ray scanners, are resolved.

If we consider that all the photons emitted by the source in a unit period of time in the direction of the detector are detected, the possible counts give rise to a discrete random variable denoted by M . It can be further shown that the probability of occurrence of M . It can be further shown that the probability of occurrence of M , at a specific value m is denoted by,

$$P_M(m) = \exp(-\lambda) \lambda^m / m! \quad (12)$$

where λ is a fixed real number.

Equation (12) is called the poisson probability law, and M which satisfies this law is called a poisson random variable with parameter λ . The main properties of this variable are as follows:

- (i) its mean is λ ,
- (ii) its standard deviation is $\sqrt{\lambda}$,
- (iii) it behaves normally if λ is (>100).

λ will be estimated by the count of the the number of photons during a particular period of unit time i.e., by a sample of the random variable. Poisson statistics imply that if we increase the sample by a factor of N , we increase the sample by a factor of N we reduce the size of the 1σ error by a factor of \sqrt{N} , where σ is the standard deviation.

A photon leaving the source in the direction of the detector, will reach the detector (without being absorbed or scattered) with a fixed probability ψ . This probability depends on the energy of the photons and the material lying on the line between the source and the detector. ψ is called the transmittance of the material (along that particular line), at that particular energy i.e., the photons which leave the source in the direction of the detector, a fraction ψ will eventually reach the detector, the rest being absorbed or scattered. The photons on reaching the detector are counted with an efficiency ϵ , which is called the efficiency of the detector.

Thus the number of photons which actually reach the detector without being absorbed or scattered, and are counted by the poisson variable with parameter $\lambda\psi\epsilon$.

As discussed earlier,

$$-\ln(N/N_0) = \int_C \mu(r, \phi) dl \approx S$$

where S is the ray sum & is the sample of a random variable such that,

$$|\mu_S + \ln(N/N_0)| < T,$$

$$\text{Where } T \approx (\phi_d \chi_d \psi_\alpha \epsilon_d)^{-1}$$

and ϕ_d is the fraction of photons leaving in the direction of the detector,

χ_d is the number of photons emitted during the period of measurement,

ψ_α is the transmittance of the material and

ϵ_d is the efficiency of the detector.

CHAPTER 3

EXPERIMENT USING SINGLE CHANNEL ANALYZER

3.1. The equipments needed for the experimental set up are:

1. NaI scintillation detector
2. Linear amplifier
3. High voltage unit
4. Low voltage unit
5. Single channel analyzer
6. Timer
7. Scaler
8. Gamma-ray source

3.2. Description of equipments:

3.2.1. SCINTILLATION DETECTOR: There are certain materials (e.g., organic, inorganic, and plastic) which emit flashes of light or scintillations when radiation passes through them. These scintillators can be used to detect any type of radiation but are most widely used for gamma-ray counting. The output of a scintillator is proportional to the incident energy, and hence can be used to identify the energy of a gamma-ray.

Radiation is absorbed in the scintillator when it strikes the material. The absorbed energy is utilized in lifting the electrons to the excited state and part of it appears as heat energy. The electrons in the excited state de-excite in a very short time, leading to the emission of light. The de-excitation time or the time constant of a scintillator varies with the material, and the decay time for commonly used scintillators is of the order of 10^{-8} .

The intensity of the emitted light is directly proportional to the energy lost by the incident particle. The emitted light flashes are amplified by a photo multiplier. The photo multiplier tube consists of a photo cathode and several dynodes, each of which is maintained at a successively higher voltage. The photo cathode is usually a thin coating of antimony-cesium on the inside surface of the photo multiplier, whereas the dynodes are antimony-cesium, silver-magnesium, or copper-beryllium. The electrons emitted by the photo cathode are amplified by releasing more electrons at each of the dynodes. The electrons from the last dynode are focused on to the anode connected to the preamplifier. The coupling of the scintillator to the photo multiplier is done by a light pipe. Normally, the scintillator is covered with a highly

reflecting material, such as MgO and Al₂O₃, to avoid loss of light pulses. The light pipe is commonly made of glass, lucite, or plexiglas. Its main purpose is to transmit efficiently the light pulses to the photo cathode of the photo multiplier tube.

The advantages of using a scintillator for detecting gamma-rays are as follows:

1: Since all the light pulses are emitted in a very short time, the scintillator integrates these into a single pulse. The height of this pulse is proportional to the incident gamma-ray energy.

2: Since the scintillator is solid, it has more atoms per unit volume than a gas-filled detector, leading to a better detection.

3: Since the time constant of the scintillator is small, its dead-time is very small, facilitating a high count rate.

4: A large scintillator increases the probability of absorbing the scattered gamma-rays, leading to an increase in photo peak efficiency.

A disadvantage in using a scintillator is the decrease in the light output with increase in the energy of the incident gamma-radiation. For example, the NaI(Tl) scintillator displays 20 percent variation in the light output per unit energy of gamma-ray over the range 0-1 MeV. The light output also varies greatly with the type of radiation. With the NaI(Tl) scintillator, electrons give a better response than alpha-particles for the same energy.

The overall efficiency of a scintillator is low because the detection process, namely, radiation cause light emission which is then reconverted into electrons at the photo cathode, is complex. Typically 300eV of energy is dissipated in the NaI(Tl) scintillator for the release of one photo electron; in an organic scintillator, the energy required is 1-5keV per photo electron. The corresponding energy for producing an ion-pair in a gas-filled detector is 30eV and in a semiconductor is 4eV.

Scintillators are many types, e.g., disk-type, right circular cylinder, and well-type.

3.2.2.LINEAR AMPLIFIER: It is an amplifier, which has three gain controls.

(i) Input attenuator, which have attenuation factors 1, 2, 5, 10, 20, & 50.

(ii) Coarse gain, which have amplification factors 0.1, 0.3, 1.

(iii) Fine gain, with an amplification 1-3. The pulse shaping provision of linear amplifier has variable integrating time constants 0.1μ sec, 0.2μ sec, 0.5μ sec, 1μ sec, 2μ sec & 5μ sec. Also it gives output pulse of amplitude 8V.

3.2.3.HIGH VOLTAGE UNIT: It is a high voltage supply of 300 to 2500V.

3.2.4.LOW VOLTAGE UNIT: It is a low voltage supply of -24 to $+24$ V.

3.2.5.SINGLE CHANNEL ANALYZER(SCA): An SCA can operate either in the integrating(INT) or differianting(DIFF) mode. In the INT. mode, the lower level(base line) of the SCA acts as the discriminating bias. In the DIFF mode, the lower level is set at E & the upper

level at $E+\Delta E$ so that only the signal with a pulse height between E & $E+\Delta E$ is counted by the scaler. The window ΔE can be continuously varied from 0 to 2V. The base line adjustable between 0.2 to 10V, Thus making it possible to resolve & identify any pulse amplitude in this range. the output of SCA is constant & of magnitude 10v.

3.2.6. TIMER: It is an ordinary counting set up to count the time required to take the counts. The factors are 10 sec, 50 sec, 100 sec, 500 sec, 1000sec.

3.2.7. SCALER: It is a counting set up to count the signals of pulse height between E & $E+\Delta E$.

3.2.8. GAMMA-RAY SOURCE: The γ -ray source used by us is ^{60}Co .

(iii) PROCEDURE TO COLLECT THE DATA: To collect the data we have to go through two steps:

1: IDENTIFICATION OF THE PHOTO PEAK OF A RADIOACTIVE SOURCE: Connect the low voltage and high voltage unit to the preamplifier of the scintillation head. Connect the output signal of the preamplifier

to the linear amplifier. Connect the amplifier output to the single channel analyzer(SCA). Connect the SCA output to the scalar through the timer. Turn on the low voltage unit, wait for a few minutes, and turn on the high voltage unit. Slowly increase the detector voltage to the value 500V. Place the source through a collimator. Set the window ΔE to 0.1V & slowly increase the base line from 0.1V. At each base line setting, for 10 sec time, collect the data. The counts will be high near the photo peak of the source.

2. COLLECTION OF THE DATA AT THE IDENTIFIED PHOTO PEAK: Set SCA at the voltage i.e. the voltage at which peak is identified of γ -ray source ^{60}Co . Using the experimental set up as in the step 1, collect the data using the object under parallel beam data collection mode.

CHAPTER 4

PROGRAM IMPLEMENTATION AND DESCRIPTION

There are various programs developed, which simulate the projected data, reconstruct images from actual or from simulated data. These programs have been written in Fortran.

4.1. COMPUTER IMPLEMENTATION OF THE CBP ALGORITHM:

The problem of reconstruction from projections is as follows:

Given $p(s;\theta)$ and, find $f(x,y)$ i.e., given discrete projection data in the form of the estimates of p for a finite number of rays; find a 2-D distribution, which is a reconstructed estimates of the unknown object.

In the case where p is sampled uniformly in both s and θ , for N angles $\Delta\theta$ apart, with each view having M equispaced rays Δs apart, we define

$$\begin{aligned} M^+ &= (M-1)/2 \\ &\quad \} M \text{ odd} \\ M^- &= -(M-1)/2 \\ M^+ &= (M/2)-1 \\ M^- &= -M/2 \quad \} M \text{ even} \end{aligned}$$

In order to ensure that the collection of rays specified by,

$$\{(m\Delta s, n\Delta\theta): M^- \leq m \leq M^+, 1 \leq n \leq N\}$$

covers the unit circles, we have,

$$\Delta\theta = \pi/N \text{ and } \Delta s = 1/M^+$$

A reconstruction algorithm which can be implemented on the digital computer is required to evaluate $f(k\Delta x, l\Delta y)$, which is a band limited approximation of the function to be reconstructed. Here $K^- \leq k \leq K^+$ & $L^- \leq l \leq L^+$, where k and l are the position of the co-ordinates of the image pixel. The definition of their upper and lower limits is similar to that of 'm'. Thus the projected data from N views & M rays is to be used to construct an image of $K \times L$ pixels. In this particular case, the image is composed of 21×21 pixels from 18 views each having 21 rays. The back projection integral is evaluated as follows:

$$f(k\Delta x, l\Delta y) \approx \Delta\theta \sum_{n=1}^N p(k\Delta x \cos\theta_n + l\Delta y \sin\theta_n)$$

For each angle θ_n , the convolved values of $p(s, \theta_n)$ for the $K \times L$ Values of s . We can either have a separate convolution for

every s' with the actual value of $q(s'-m\Delta s)$ at that point or we can evaluate $p(m\Delta s, \theta_n)$ only within the specified limits of m & then use interpolation. The latter approach is much faster and cheaper. These operations are represented by,

$$p_c(m\Delta s, \theta_n) \approx \Delta s \sum_{m=M^-}^{M^+} p(m\Delta s, \theta_n) q(m-m\Delta s), \quad M^- \leq m \leq M^+$$

$$p_I(s', \theta_n) \approx \Delta s \sum_m p_c(m\Delta s, \theta_n) I(s-m\Delta s)$$

where $I(s)$ is an interpolating function. A linear interpolating function, say $I(s)$, corresponding to linear interpolation between adjunct samples is

$$I_L(s) = \begin{cases} 0, & |s| \geq \Delta s \\ 1/\Delta s (1 - |s|/\Delta s), & |s| \leq \Delta s \end{cases}$$

using the above formulae, a program was written in FORTRAN to implement the CBP algorithm.

4.2. PROGRAM FOR RECONSTRUCTING THE IMAGE FROM DATA:

The program (see appendix B) can reconstruct an image from experimental data. The program is written in Fortran to accept the

data for the parallel beam geometry and use to reconstruct the image. Images of several experiments are reconstructed within acceptable error limits.

A suitable image quality index would be helpful in quantitatively estimating the accuracy of image reconstruction. Two such indices are I_1 and I_2 . The process of reconstruction can be terminated if the error of reconstruction reaches a certain minimum value. The actual program details are follows:

1. The parameters of the program LITM(the number of rays per projection) and LITP(parallel beam data) are read in from data file.
2. The projected data are read in from a data file. This transformation enables us to use the CBP algorithm, for parallel beam data, without resorting to the Hilbert transform.
3. The Ramchandran- Lakshminarayan filter is used in this program. The numerical values had been computed and stored in a file. These values were merely read from the file into an array. It is at this stage that the convolution is carried out.

Convolution is especially easy if the values to be convolved are stored in an array. It is often found that, during back-projection of data, the the convolved values do not exactly pass through the point being reconstructed. Due to this interpolation has to be used. Since linear interpolation is fast and it gives good results, it has been used in this particular implementation.

4. The superimposition of these interpolated values is carried out. Some convenience like display of point values as they are reconstructed have been added to the program. These reconstructed values are the LITF values.

A sample output of this program has been displayed in appendix C.

CHAPTER 5

RESULTS

In this chapter, the results obtained with the actual experimental data have been presented.

5.1. DATA USED: The data used are taken from the study conducted by us using single channel analyzer(SCA). The details are briefly summarized as follows:

- a) The source of nuclear radiation is 1.33 Mev of Co-60. The collimator is fixed at the other end. The source and detector are placed at the fixed place but the object is moved, perpendicularly to the axis of the collimator, which covers the whole outer diameter of the object, because of parallel beam formulation.
- b) The detector is connected to the other end of the collimator and the subsequent stages being an amplifier, single channel analyzer, a timer and a scaler.
- c) The settings of the apparatus are:
Polarity is = -ve,

Attenuator = 20,
Gain = 0.16,
High voltage = 1000V,
Lower level of window = 0.5V,
Window width = 0.1V.

d) The data collected for calibration are for a cylinder, a small cylinder in a large cylinder, and water in beaker. Raw data appears in Appendix A.

5.2. RESULTS: The reconstruction results are given in Fig 4-9.

The results shows that we can reconstruct the image of the object of any shape and sort out the defects in the object through nondestructive testing. We calculate the void fraction during a "LOSS OF COOLANT ACCIDENT"(LOCA). We can measure cross-sectional distribution of any property through indirect measurement by probing the object with invisible, penetrating radiation and interpretation of these results.

Expression (13) in section 2.6 shows that the error in measurements depends on various different factors and it may be reduced by ,

NEGATIVE IMAGE

image data1 (hollow cylinder)

ram257

```

23 23 23 23 23 23 23 23 23 23 36 23 23 23 23 23 23 23 23 23
23 23 23 23 23 23 66 90 99 90 79 66 54 49 44 23 23 23 23 23
23 23 23 23 23 87 85 56 43 42 48 58 64 60 41 23 20 23 23 23
23 23 23 54 93 56 29 32 33 33 32 33 40 54 80 71 39 32 23 23
23 23 23 93 48 31 33 32 31 29 27 29 31 33 37 66 78 39 31 23 23
23 23 84 53 27 30 27 20 13 15 18 21 23 29 33 33 66 73 36 23 23
23 59 84 29 33 32 20 18 30 29 24 21 22 24 29 36 40 84 55 33 23
23 84 54 33 34 26 23 38 26 19 16 8 6 13 19 28 32 55 73 36 23
23 92 36 32 30 20 32 24 19 28 36 39 18 4 12 21 30 37 80 40 23
23 88 27 30 26 15 31 10 16 17 27 48 50 11 14 21 31 33 80 46 23
39 86 26 31 24 16 28 8 13 8 0 49 61 21 17 23 34 35 80 49 30
23 91 30 34 29 18 34 13 19 20 30 51 53 14 17 24 34 36 83 49 23
23 95 38 35 32 22 35 27 22 30 38 41 20 6 15 24 32 39 82 42 23
23 82 52 31 32 23 20 36 24 16 13 6 4 11 17 25 30 52 71 33 23
23 56 81 26 30 29 18 15 27 27 21 19 19 21 26 33 37 81 52 30 23
23 23 86 55 29 32 30 23 16 17 21 24 25 32 35 36 68 76 38 23 23
23 23 45 93 48 31 33 32 31 29 27 29 31 33 37 67 78 40 32 23 23
23 23 23 53 93 56 29 31 32 32 32 33 39 54 79 71 39 32 23 23 23
23 23 23 23 54 98 97 67 54 53 59 69 75 71 52 35 32 23 23 23 23
23 23 23 23 23 23 48 71 81 71 61 48 36 30 25 23 23 23 23 23 23
23 23 23 23 23 23 23 23 23 23 42 23 23 23 23 23 23 23 23 23

```

MINIMUM LITF=-0.40044650E+00MAXIMUM LITF= 0.13052070E+01

HORIZONTAL CENTERLINE

```

1 11 0.21168850E+00
2 11 0.96284930E+00
3 11 0.42147220E+00
4 11 0.15797270E+00
5 11 0.64991230E-01
6 11 -0.83049510E-01
7 11 0.18420810E-01
8 11 -0.13323200E+00
9 11 0.21875770E+00
10 11 0.63131760E-01
11 11 -0.40044650E+00
12 11 0.11658500E+00
13 11 0.26064080E+00
14 11 -0.17348870E+00
15 11 -0.30801080E-01
16 11 -0.40010730E-01
17 11 0.67800190E-01
18 11 0.15288580E+00
19 11 0.61488460E+00
20 11 0.64471690E+00
21 11 0.31587560E+00

```

AVERAGE = 0.28368430E+00

Fig. 4

NEGATIVE IMAGE

image data2 (hollow cylinder)

ram257

```

6 6 6 6 6 6 6 6 6 6 17 6 6 6 6 6 6 6 6 6
6 6 6 6 6 6 50 79 89 78 64 50 40 32 27 6 6 6 6 6
6 6 6 6 6 90 90 58 43 35 36 36 32 25 12 3 1 6 6 6
6 6 6 41 91 55 26 25 25 27 31 41 48 50 43 27 7 1 6 6 6
6 6 6 91 43 20 18 10 6 5 6 7 13 34 59 56 37 14 7 6 6
6 6 80 50 19 14 3 4 9 13 14 18 18 12 19 58 59 34 11 6 6
6 46 81 19 16 3 5 10 9 8 7 8 12 22 18 21 65 52 25 10 6
6 77 47 18 7 3 10 9 5 4 4 3 4 9 21 15 38 64 40 13 6
6 90 28 17 3 9 10 6 8 12 9 9 5 4 13 22 19 65 47 17 6
6 88 20 14 1 10 8 4 11 0 4 2 9 2 7 22 11 59 53 19 6
26 87 19 13 2 11 8 5 10 2 51 7 10 4 7 22 12 56 56 25 11
6 88 20 14 1 10 9 5 12 0 5 2 9 2 7 22 12 60 53 20 6
6 89 28 17 2 9 10 6 7 11 9 9 5 3 12 21 18 64 47 17 6
6 77 47 18 7 3 10 9 5 4 4 3 4 9 21 15 37 64 40 13 6
6 46 81 19 16 3 5 10 8 8 7 8 12 22 18 21 65 52 25 10 6
6 6 82 52 21 16 6 6 12 15 16 20 20 15 21 60 61 36 13 6 6
6 6 30 91 44 20 18 11 6 6 7 7 14 34 60 56 38 15 7 6 6
6 6 6 49 99 63 34 32 32 34 39 48 56 57 51 34 14 9 6 6 6
6 6 6 6 36 90 91 58 43 36 37 36 33 25 13 3 1 6 6 6 6
6 6 6 6 6 6 29 59 68 57 44 29 19 12 7 6 6 6 6 6 6
6 6 6 6 6 6 6 6 6 6 25 6 6 6 6 6 6 6 6 6 6

```

MINIMUM LITF=-0.66823720E-01 MAXIMUM LITF= 0.11211560E+01

HORIZONTAL CENTERLINE

```

1 11 0.13578740E+00
2 11 0.70373300E+00
3 11 0.36659040E+00
4 11 0.31033430E+00
5 11 0.83562060E-02
6 11 0.10504080E+00
7 11 0.18786710E-01
8 11 -0.19490020E-01
9 11 0.42055060E-01
10 11 -0.15771860E-01
11 11 0.54551830E+00
12 11 -0.10842180E-01
13 11 0.37594020E-01
14 11 -0.21192550E-01
15 11 0.17795910E-01
16 11 0.13091370E+00
17 11 0.11964570E-01
18 11 0.40251220E+00
19 11 0.37126590E+00
20 11 0.45639540E+00
21 11 0.23131480E+00

```

AVERAGE = 0.25251840E+00

Fig. 5

NEGATIVE IMAGE

image data3 (water in a beaker)

ram257

```

0 0 0 0 0 0 0 0 0 0 0 50 0 0 0 0 0 0 0 0 0
0 0 0 0 0 0 40 47 49 56 56 60 65 66 62 0 0 0 0 0 0
0 0 0 0 0 52 56 59 63 59 58 53 49 52 64 71 64 0 0 0 0
0 0 0 30 43 47 49 51 52 57 67 79 84 73 50 51 67 62 0 0 0
0 0 0 57 61 62 63 75 79 72 58 45 45 67 97 76 59 79 72 0 0
0 0 49 57 57 64 82 71 52 48 52 56 50 31 28 79 64 46 66 0 0
0 39 53 57 59 81 60 40 46 46 47 51 59 66 46 33 90 48 65 65 0
0 47 55 58 75 69 42 48 43 41 39 35 39 55 68 37 55 79 54 70 0
0 49 56 57 79 47 43 40 38 46 61 59 41 38 57 58 29 87 46 69 0
0 51 55 60 77 37 41 32 36 72 84 96 71 40 56 70 27 86 54 68 0
32 49 54 62 73 35 39 29 40 71 15 99 83 45 55 71 31 83 58 72 61
0 54 57 62 79 39 43 35 38 74 86 98 73 42 58 72 30 88 56 70 0
0 52 58 60 82 50 45 43 41 49 64 62 44 41 59 61 32 90 49 72 0
0 45 54 56 74 67 40 46 42 39 37 33 37 53 66 35 53 77 52 68 0
0 41 55 58 61 82 61 41 48 48 48 52 60 68 47 34 91 49 66 67 0
0 0 53 61 61 68 86 75 56 52 56 60 54 35 32 83 68 50 70 0 0
0 0 28 43 48 48 50 62 66 59 44 32 32 53 84 62 45 66 59 0 0
0 0 0 42 55 59 61 63 64 69 79 91 96 85 62 63 79 74 0 0 0
0 0 0 0 34 46 51 53 57 53 52 48 43 46 59 65 59 0 0 0 0
0 0 0 0 0 0 46 52 54 61 61 65 70 71 67 0 0 0 0 0 0 0
0 0 0 0 0 0 0 0 0 0 0 53 0 0 0 0 0 0 0 0 0 0

```

MINIMUM LITF= 0.00000000E+00 MAXIMUM LITF= 0.44662020E+00

HORIZONTAL CENTERLINE

1	11	0.22416400E+00
2	11	0.25203760E+00
3	11	0.26107460E+00
4	11	0.30184300E+00
5	11	0.26093440E+00
6	11	0.23663320E+00
7	11	0.21235230E+00
8	11	0.17549860E+00
9	11	0.27727590E+00
10	11	0.37964080E+00
11	11	0.66363890E-01
12	11	0.38910240E+00
13	11	0.28998650E+00
14	11	0.16754630E+00
15	11	0.21807630E+00
16	11	0.25424100E+00
17	11	0.20030450E+00
18	11	0.35631680E+00
19	11	0.23613930E+00
20	11	0.27548370E+00
21	11	0.24020260E+00

AVERAGE = 0.25685540E+00

Fig. 6

NEGATIVE IMAGE

image data 4 (water in beaker)

ram257

```

0 0 0 0 0 0 0 0 0 0 29 0 0 0 0 0 0 0 0 0
0 0 0 0 0 0 34 45 46 48 49 48 40 35 30 0 0 0 0 0
0 0 0 0 0 40 48 50 48 52 53 57 59 56 47 36 20 0 0 0
0 0 0 37 47 50 51 52 54 55 54 49 46 49 60 58 44 25 0 0
0 0 0 46 52 53 57 68 76 77 76 77 74 62 42 52 57 41 20 0
0 0 38 46 46 52 67 55 40 33 38 47 61 74 77 44 50 56 37 0
0 34 48 51 52 69 51 32 35 36 33 25 26 51 76 79 46 66 50 31
0 43 50 51 67 61 36 43 58 64 62 59 41 13 45 77 65 47 57 35
0 44 49 50 69 40 37 53 53 43 48 55 61 40 18 58 79 42 60 40
0 53 55 61 75 42 49 70 55 78 56 32 53 59 15 51 83 46 62 49
36 49 55 63 73 42 54 72 67 99 47 5 32 51 8 37 74 42 54 40
0 46 48 54 68 35 42 63 48 71 49 25 46 52 8 44 76 39 55 42
0 46 51 53 72 43 40 56 56 45 51 58 64 43 21 61 81 44 63 43
0 42 49 50 66 60 35 42 57 63 61 58 40 12 44 76 64 46 56 34
0 29 43 47 47 65 46 28 30 31 29 20 22 47 72 75 42 62 46 27
0 0 43 51 51 57 72 61 45 38 43 53 66 79 82 50 56 62 43 0
0 0 36 47 52 53 57 69 76 77 76 78 75 62 43 53 58 42 21 0
0 0 0 34 43 47 48 49 50 51 51 46 43 45 57 54 41 22 0 0
0 0 0 0 35 44 51 53 52 56 57 61 62 60 51 40 24 0 0 0
0 0 0 0 0 0 32 43 44 46 46 46 38 33 28 0 0 0 0 0
0 0 0 0 0 0 0 0 0 0 28 0 0 0 0 0 0 0 0 0

```

MINIMUM LITF= 0.00000000E+00 MAXIMUM LITF= 0.51089570E+00

HORIZONTAL CENTERLINE

1	11	0.14889710E+00
2	11	0.25077410E+00
3	11	0.27300830E+00
4	11	0.27929180E+00
5	11	0.39062360E+00
6	11	0.19361240E+00
7	11	0.17229710E+00
8	11	0.32027630E+00
9	11	0.24780840E+00
10	11	0.28737710E+00
11	11	0.24160640E+00
12	11	0.25114970E+00
13	11	0.26126380E+00
14	11	0.31593150E+00
15	11	0.15010590E+00
16	11	0.22060840E+00
17	11	0.39419930E+00
18	11	0.26167260E+00
19	11	0.29198520E+00
20	11	0.23948220E+00
21	11	0.14241280E+00

AVERAGE = 0.25651930E+00

Fig. 7

NEGATIVE IMAGE

image data 5 (small cylinder in a large cylinder)

ram257

```

19 19 19 19 19 19 19 19 19 19 19 38 19 19 19 19 19 19 19 19 19 19
19 19 19 19 19 19 21 21 28 45 56 66 74 67 43 19 19 19 19 19 19
19 19 19 19 19 30 50 77 86 80 70 64 64 74 95 92 56 19 19 19 19
19 19 19 30 40 82 98 69 49 39 33 30 29 31 37 61 85 53 19 19 19
19 19 19 38 89 82 46 31 24 23 26 27 27 24 22 28 49 81 42 19 19
19 19 33 80 80 38 22 18 21 23 24 26 30 31 30 24 30 57 76 19 19
19 27 48 95 42 19 16 18 17 23 28 28 28 30 33 32 26 36 78 53 19
19 29 83 66 27 17 18 19 39 48 47 47 42 32 33 36 32 31 57 78 19
19 39 99 51 24 22 24 47 58 48 32 22 33 37 29 33 34 28 44 86 19
19 44 96 38 17 21 26 57 50 18 18 27 12 34 23 27 30 23 33 82 19
32 45 94 36 17 20 29 57 39 0 5 39 19 36 28 29 33 26 34 81 42
19 47 99 41 20 24 29 60 53 21 21 30 15 37 26 30 33 26 36 85 19
19 34 94 46 19 17 19 42 54 43 27 17 28 32 24 28 29 23 39 81 19
19 29 82 65 26 16 17 18 38 48 47 46 42 31 32 35 31 31 57 78 19
19 29 50 97 44 21 18 19 19 24 30 29 30 32 35 33 27 38 79 55 19
19 19 34 82 82 40 24 19 23 25 26 27 31 32 32 26 32 59 78 19 19
19 19 29 40 90 84 48 33 26 25 28 29 29 26 24 30 51 82 44 19 19
19 19 19 25 35 78 93 65 45 34 29 26 25 27 33 56 81 49 19 19 19
19 19 19 19 16 19 39 66 74 69 59 52 53 63 84 81 45 19 19 19 19
19 19 19 19 19 19 40 39 47 63 75 84 92 86 62 19 19 19 19 19 19
19 19 19 19 19 19 19 19 19 19 33 19 19 19 19 19 19 19 19 19 19

```

MINIMUM LITF=-0.28042350E+00MAXIMUM LITF= 0.12123950E+01

HORIZONTAL CENTERLINE

1	11	0.29664600E+00
2	11	0.56507520E+00
3	11	0.77331440E+00
4	11	0.22086830E+00
5	11	0.10714460E+00
6	11	0.85287780E-01
7	11	0.13926930E+00
8	11	0.42794420E+00
9	11	0.19981520E+00
10	11	-0.60724200E-02
11	11	-0.20450700E+00
12	11	0.38276980E-01
13	11	0.12662600E+00
14	11	0.42128090E+00
15	11	0.16544220E+00
16	11	0.10876240E+00
17	11	0.13471620E+00
18	11	0.15594940E+00
19	11	0.60249870E+00
20	11	0.84551330E+00
21	11	0.21986170E+00

AVERAGE = 0.35917920E+00

Fig. 8

NEGATIVE IMAGE

image data 6(small cylinder in a large cylinder)

ram257

```

11 11 11 11 11 11 11 11 11 11 37 11 11 11 11 11 11 11 11 11
11 11 11 11 11 11 45 45 47 41 37 29 27 28 42 11 11 11 11 11
11 11 11 11 11 53 56 57 55 56 53 49 42 31 14 13 42 11 11 11
11 11 11 55 59 63 66 67 68 66 62 58 53 47 40 22 4 32 11 11
11 11 11 55 59 62 65 60 57 55 58 65 69 61 49 39 22 0 33 11
11 11 53 58 62 62 53 50 51 56 58 56 56 68 73 57 43 23 8 11
11 49 55 57 59 51 45 52 66 73 77 85 82 62 64 77 54 40 9 27
11 51 56 59 53 44 49 66 59 55 55 57 72 95 67 74 73 51 28 15
11 56 58 61 49 48 66 63 62 64 54 55 54 72 90 66 80 57 39 9
11 55 59 62 49 51 71 62 71 39 30 23 48 51 91 62 80 61 41 6
50 58 61 61 49 55 73 65 68 39 99 20 40 47 87 65 78 63 42 9
11 54 58 60 48 49 70 61 69 37 29 22 46 49 89 60 78 60 40 5
11 54 56 59 48 46 64 61 61 63 52 54 52 70 89 64 78 55 38 8
11 51 56 59 53 44 49 66 59 55 55 57 72 95 67 74 73 51 28 15
11 53 59 61 64 55 49 56 70 77 81 89 86 66 68 81 58 44 13 31
11 11 53 58 62 62 52 50 51 56 57 56 56 68 73 57 43 23 8 11
11 11 54 59 64 67 69 64 61 60 63 70 73 66 54 44 27 5 37 11
11 11 11 50 55 59 61 63 64 62 58 53 49 43 35 18 0 27 11 11
11 11 11 11 46 49 53 53 52 52 49 46 39 27 11 10 39 11 11 11
11 11 11 11 11 11 36 36 38 32 29 20 18 19 33 11 11 11 11 11
11 11 11 11 11 11 11 11 11 11 43 11 11 11 11 11 11 11 11 11

```

MINIMUM LITF=-0.61044890E-01MAXIMUM LITF= 0.48694250E+00

HORIZONTAL CENTERLINE

```

\
1 11 0.14145230E+00
2 11 0.14603000E+00
3 11 0.23134540E+00
4 11 0.28290670E+00
5 11 0.26219300E+00
6 11 0.25808520E+00
7 11 0.36757640E+00
8 11 0.24262980E+00
9 11 0.23847800E+00
10 11 0.10660200E+00
11 11 0.48694250E+00
12 11 0.98800910E-01
13 11 0.22883360E+00
14 11 0.24277430E+00
15 11 0.38989580E+00
16 11 0.25710580E+00
17 11 0.28732000E+00
18 11 0.25873290E+00
19 11 0.21273050E+00
20 11 0.97292160E-01
21 11 0.17499630E+00

```

AVERAGE = 0.22804870E+00

Fig. 9

1. Increasing the strength of the source or the time period of measurements.

2) Improving the efficiency of the detector.

The projection for the objects are assumed to be less affected by statistical errors since averaging over a large number of readings has been carried out.

The detector for photon detection has been collimated to accept only those photons which come straight from the source. However, perfect collimation is difficult to achieve. This allows some scattered radiation to enter the collimator window, artificially boosting the counts. Since only straight attenuation photons are related to the chordial density, scattered photons produce an overestimate of the density(LITF). These effects due to photon scattering have not been taken into account. The increased number of counts due to scatter will not results in an overestimate of $\langle \alpha \rangle$ if the effect of scattered photons is the along all chordial directions. This is a fairly strong assumption and may not be always valid. It has possibly resulted in underestimates of density (LITF), partially compensating for the greater effects of counting statistics at lower counts.

CHAPTER 6

CONCLUSION AND RECOMMENDATION

It has been observed in the course of study that image reconstructed can be extended to get the meaningful results for measurements of void fraction in a multiphase flow. It is also possible to have LITF to be identical to μ , the attenuation constant of the material at that energy, by suitably normalizing the input data and ensuring that the same system of units is consistent during computation.

The error in reconstruction occurs due to the error incorporated in the projection data, and the error in the projection data occurs due to counting of scattered photons.

The results also shows that the error occurs due to imperfect collimation of the source and the poor activity of the source. The accessibility of the experiment can also be extended by use of automatic system, which can be done by use of feedback using PC.

It is apparent from the above recommendations that further investigations are needed along these lines. Besides, the study is conducted using only Ramchandran- Lakshminarayan filter.

Investigation for other window functions can be carried out using limited amount of data. A larger number of rays will also give a better results. Of course this work has been done earlier using automatic system but whatever we have done using manual system gives good results as comparable to the automatic system.

REFERENCES

1. P. Munshi, "Two phase flow studies in the bubbly flow regime using a scanning Gamma-ray densitometer", Master of science thesis, Ohio state university, (1979).
2. J. Radon, "Über die bestimmung von funktionen durch ihre integral werte langs gewisser Maaniggfaltigkeiten", Berichte sachsische akademie der wissenschaften leipzig, Math-Phys. Kl., 69(1917), pp. 262-267.
3. A. M. Cormack, "Representation of a function by its line integrals with some Radiological applications" J. Appl. Phys., 35(1964), pp. 195-207.
4. G. T. Herman, "Image reconstruction from projections: The fundamentals of Computerized Tomography", Academic press, New York (1980).
5. P. Munshi, "Error estimates for the convolution back projection algorithm in Computerized Tomography", Doctor of philosophy, thesis, IIT Kanpur, (1989).

51 CENTRAL LIBRARY

acc. No. **A113494**

6. A. Mackovski, "Physical problems of computerized tomography", Proceedings of the IEEE, 71 No.3, (1983), pp. 373-378.
7. L. A. Shepp and B.F.Logan, "The Fourier reconstruction of head section", IEEE Trans. Nucl. Sci, NS-21 (1974), pp. 21-43.
8. "CT Scanners for Butchers', Science Today, 22, 3(1988), p.26.
9. G.N.Ramchandran, A.V.Lakshminarayan,"3-D reconstruction from Radiograph and Micrographs; Application of convolution instead of Fourier Transforms", Proceeding National. Academy Science, USA, 68, 1971, pp. 2236-2240.
10. R.M.Lewitt, "Reconstruction algorithm: Transform methods", Proceeding IEEE, 71 No.3 (1983), pp. 390-408.
11. Mahesh Vaidya, "A study of the poisson errors in the convolution backprojection algorithm for computerized tomography," M. Tech. Thesis, I.I.T. Kanpur (1991).
12. R.N. Bracewell, A.C. Riddle, "Inversion of fan beam scans in radio astronomy", Astrophys. J. 150, (1967) pp. 427-434.

APPENDIX A

Lower level voltage	Counts per 10 secs
0.0	76
0.1	30
0.2	27
0.3	27
0.4	26
0.5	25
0.6	26
0.7	29
0.8	29
0.9	39
1.0	47
1.1	50
1.2	53
1.3	53
1.4	51
1.5	68
1.6	61
1.7	53
1.8	51
1.9	49
2.0	48
2.1	48
2.2	51
2.3	66
2.4	72(photo peak)
2.5	58
2.6	52
2.7	47

OBJECT 1.
HOLLOW CYLINDER

DISTANCE MOVED BY OBJECT(cms.)	COUNTS PER 50 SECS	
	SCAN 1	SCAN 2.
AIR	1637	1648
0.0	1545	1532
0.5	702	745
1.0	874	893
1.5	977	950
2.0	1118	1123
2.5	1124	1153
3.0	1134	1143
3.5	1179	1198
4.0	1154	1165
4.5	1205	1234
5.0	1114	1136
5.5	1184	1167
6.0	1146	1178
6.5	1152	1186
7.0	1070	1076
7.5	986	974
8.0	994	1004
8.5	788	796
9.0	1065	1076
9.5	1486	1478
10.0	1602.	1611

OBJECT 2		
WATER IN A BEAKER		
DISTANCE MOVED BY OBJECT(cms.)	COUNTS PER 50 SECS.	
	SCAN 1	SCAN 2.
AIR	951	941
0.0	814	851
0.4	727	687
0.8	656	642
1.2	627	572
1.6	628	596
2.0	620	591
2.4	573	554
2.8	565	557
3.2	548	528
3.6	575	556
4.0	562	586
4.4	594	566
4.8	568	577
5.2	560	627
5.6	539	565
6.0	609	666
6.4	620	671
6.8	715	775
7.2	808	879
7.6	890	849
8.0	812.	852

OBJECT 3.
SMALL CYLINDER IN A HOLLOW CYLINDER

DISTANCE MOVED BY THE OBJECT(cms.)	COUNTS PER 50 SECS	
	SCAN 1	SCAN 2.
AIR	941	945
0.0	885	846
0.5	782	745
1.0	328	335
1.5	446	403
2.0	506	525
2.5	536	566
3.0	527	581
3.5	488	466
4.0	475	451
4.5	478	539
5.0	566	549
5.5	534	515
6.0	587	554
6.5	446	502
7.0	433	543
7.5	604	526
8.0	499	520
8.5	558	541
9.0	455	459
9.5	362	393
10.0	765	812.

APPENDIX B

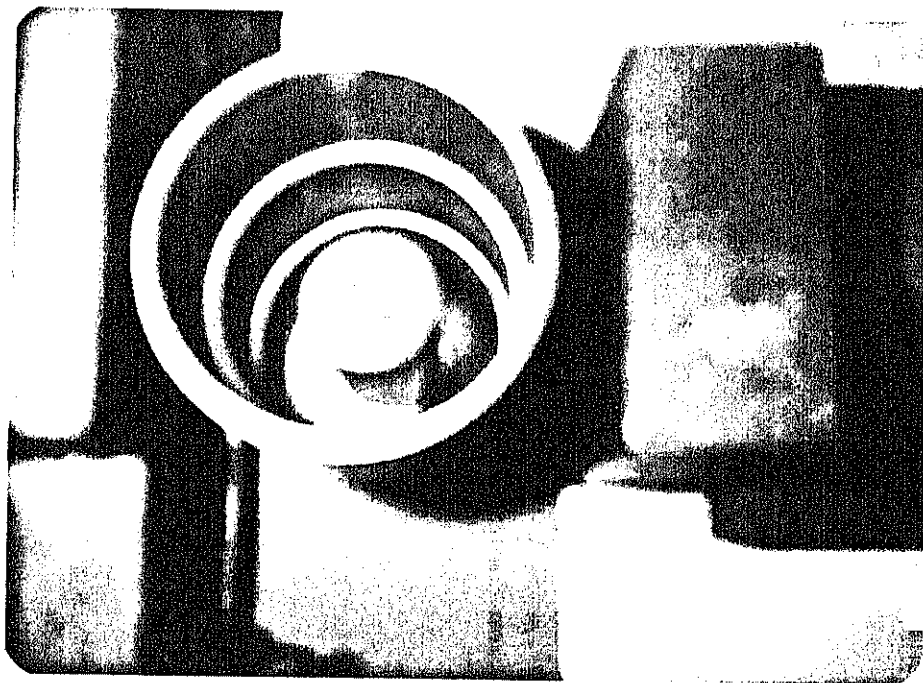


Oject 1.
Hollow cylinder

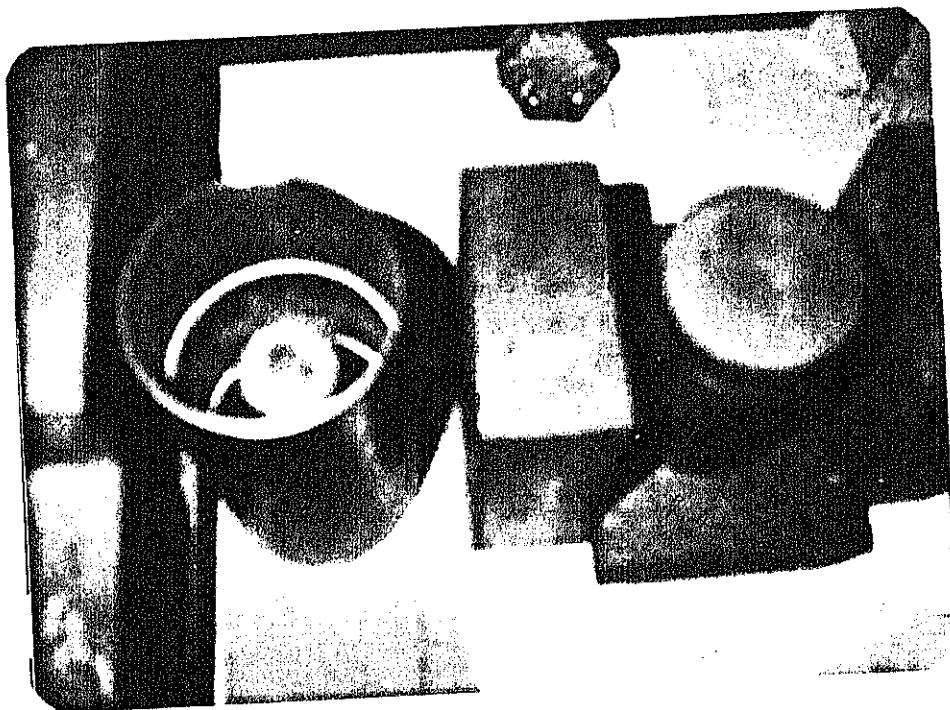


Object 2.
Water in a beaker





Object 3.
Small cylinder in
a large cylinder



APPENDIX C

```

C      PROGRAM FOR THE RECONSTRUCTION OF THE IMAGE
C      N--NUMBER OF PROJECTIONS IN SCAN (PARALLEL)
C      M--NUMBER OF RAYS PER VIEW (FAN BEAM)
C      LITN--NUMBER OF PROJECTIONS IN SCAN(FAN BEAM)
C      LITM--NUMBER OF RAYS PER PROJECTION(PARALLEL)
C      LITH--FAN BEAM DATA (ARRAY WITH M+1 BY LITN+1 ELEMENTS)
C      D--DISTANCE FROM SOURCE TO CENTRE OF OBJECT
C      T--DIAMETER OF OBJECT
C      LAMMAX--MAXIMUM POSSIBLE VALUE OF LAMBDA
C      LITA--DISTANCE BETWEEN PARALLEL RAYS IN EACH VIEW
C      ALPHA--ANGULAR SPACING BETWEEN PARALLEL VIEW(RADIANS)
C      LITP--PARALLEL BEAM DATA(ARRAY WITH LITM+1 BY N+1 ELEMENTS)
C      LITW--FILTER FUNCTION DATA(ARRAY WITH LITM+1 ELEMENTS)
C      LITC--CONVOLUTED DATA(ARRAY WITH LITM+1 BY N+1 ELEMENTS)
C      LITF--BACK-PROJECTED DATA (ARRAY WITH LITM+1 ELEMENTS)
C      DELLAM--SPACING BETWEEN FAN BEAMS(IN TERMS OF LAMBDA)
C
C      REAL LITP(50,91),LITW(50),SUM,LITC(50,91),LITF(50,50),T,THETA
C      REAL YY,Z,Y(50),X(50),SPRIME,LITR
C      INTEGER LITM,N,J,K,L,TITLE(20),TTL(20)
C      INTEGER FILCBP,DATA,CONVLV,PRINT,ANS,PRT,XMAX,YMAX
C      INTEGER M,LINE(50)
C
C      FILE NUMBER VARIABLES
C20
C      FILCBP=1
C      DATA=2
C      CONVLV=3
C      PRINT=4
C      PIE=4.*ATAN(1.)
C      OPEN(UNIT=DATA,FILE='CBPPM.DAT')
C      READ(DATA,*)NRAY,NANGLE
C
C      READ PARALLEL DATA
C
C      11  FORMAT(64A1)
C          DO 40 K=1,NANGLE
C      OPEN(UNIT=DATA,FILE='PROJ21.DAT')
C      READ(DATA,11) (TITLE(I),I=1,20)
C      READ(DATA,*) (LITP(J,K),J=1,NRAY)
C      CLOSE(UNIT=DATA)
C      40  CONTINUE
C
C      E=1.0
C      CONS=E
C      PIXSP= 2.0*E/(NRAY-1)
C      DELTH=PIE/NANGLE
C      XMAX=NRAY-1
C      YMAX=NRAY-1

```

```

C      READ FOURIER FILTER
C
OPEN(UNIT=FILCBP,FILE='FILCBP.DAT')
READ(FILCBP,11) (TTL(I),I=1,20)
READ(FILCBP,*) (LITW(K),K=1,NRAY)
      DO 30 K=1,NRAY
LITW(K)=LITW(K)/(PIXSP*PIE)
30    CONTINUE
CLOSE(UNIT=FILCBP)

C
C
C      COMPUTE CONVOLUTION
C30
      DO 70 K=1,NANGLE
      DO 60 L=1,NRAY
      LITC(L,K)=0.0
      DO 50 J=1,NRAY
      LITC(L,K)=LITC(L,K)+(LITP(J,K)*LITW(ABS(L-J)+1))
50    CONTINUE
60    CONTINUE
WRITE(5,*)K
70    CONTINUE
C
C      THIS PROGRAM BACK PROJECTS THE TOMOGRAPHY DATA
C
C      CALCULATE SUPERIMPOSITION OF DATA
C
X(1)=-CONS
Y(1)=-CONS
DO 110 I=2,NRAY
X(I)=X(I-1)+PIXSP
Y(I)=Y(I-1)+PIXSP
110  CONTINUE
SUM1=0.0
NUMBER=0
DO 312 K=1,NRAY
DO 312 L=1,NRAY
LITF(K,L)=0.0
312  CONTINUE
DO 120 K=1,NRAY
DO 120 L=1,NRAY
SUM=0.0
DO 130 J=1,NANGLE
AX=X(K)
AY=Y(L)
THETA=FLOAT(J-1)*PIE/FLOAT(NANGLE)
QTY=(AX*AX+AY*AY)
LITR=SQRT(QTY)
IF(LITR.GT.1.0) GO TO 120
SPRIME=(X(K)*COS(THETA)+Y(L)*SIN(THETA))/PIXSP
G=SPRIME+FLOAT(NRAY/2+1)
M=IFIX(FLOOR(G))
IF(M.GT.NRAY) LITC(M+1,J)=0.0
SUM=SUM+(FLOAT(M+1)-G)*LITC(M,J)+(G-FLOAT(M))*LITC(M+1,J)
130  CONTINUE
SUM=SUM*DELTH
LITF(K,L)=SUM
SUM1=SUM1+LITF(K,L)

```



```

120      CONTINUE
      AVE=SUM1/NUMBER
      WRITE(*,*) AVE

C
C      THIS PROGRAM PRINTS THE TOMOGRAPHY DATA
C
C      PRINT DATA
C40
      YY=99999.0
      Z=-99999.0
          DO 230 L=1,XMAX+1
          DO 220 J=1,YMAX+1
      YY=MIN(YY,LITF(L,J))
      Z=MAX(Z,LITF(L,J))
220      CONTINUE
230      CONTINUE
C      WRITE(*,35)
C35     FORMAT('NEGATIVE OF IMAGE?(0=NO,1=YES)')
C      ACCEPT *,ANS
C      WRITE(*,36)
C36     FORMAT('OPRINT IMAGE ON TERMINAL?(0=NO,1=YES)')
C      ACCEPT *,PRT
      ANS=1
      PRT=1
C      OPEN PRINT FILE
      OPEN(UNIT=PRINT,FILE='RESULTS.DAT')
      IF(ANS.EQ.1) WRITE(PRINT,37)
37      FORMAT('NEGATIVE IMAGE')
      IF(ANS.NE.1) WRITE(PRINT,39)
39      FORMAT('POSITIVE IMAGE')
      WRITE(PRINT,38) (TITLE(I),I=1,20)
      WRITE(PRINT,38) (TTL(I),I=1,20)
38      FORMAT(20A1)
      DO 250 L=1,XMAX+1
          DO 240 J=1,YMAX+1
              LINE(J)=IFIX(0.5+99.0*(LITF(L,J)-YY)/(Z-YY))
              IF(ANS.NE.1) LINE(J)=99-LINE(J)
240      CONTINUE
      WRITE(PRINT,45) (LINE(M),M=1,YMAX+1)
45      FORMAT(25I3)
      IF(PRT.EQ.1) WRITE(*,45) (LINE(M),M=1,YMAX+1)
250      CONTINUE
C      WRITE(PRINT,260) YY,Z
260      FORMAT(/'MINIMUM LITF=',E15.8,'MAXIMUM LITF=',E15.8)
      IF(PRT.EQ.1) WRITE(*,260) YY,Z
      IF(PRT.EQ.1) WRITE(PRINT,260) YY,Z
C      PRINT CENTER LINES OF PROJECTION
      WRITE(PRINT,102)
102     FORMAT('HORIZONTAL CENTERLINE'/)
      JC=XMAX/2+1
          DO 112 I=1,XMAX+1
              WRITE(PRINT,122) I,JC,LITF(I,JC)
122     FORMAT(1X,I3,2X,I3,5X,E15.8)
112     CONTINUE
      WRITE(*,*) ((LITF(I,J),J=JC,JC),I=1,NRAY)
      WRITE(PRINT,77) AVE
77      FORMAT(/' AVERAGE =',E15.8)
C50     CLOSE LISTING FILE

```

```
CLOSE (UNIT=PRINT)  
STOP  
END
```

C

```
FUNCTION FLOOR(A)  
REAL A  
FLOOR=IFIX(A)  
IF(FLOOR.GT.A) FLOOR=FLOOR-1.0  
RETURN  
END
```

C

A113494

NETP-1992 - M - DWI - EXP